ELSEVIER

Biochimica et Biophysica Acta 1515 (2001) 189–201

BIOCHIMICA ET BIOPHYSICA ACTA

BBA

www.bba-direct.com

La^{3+} stabilizes the hexagonal II (H_{II}) phase in phosphatidylethanolamine membranes

Tomoki Tanaka [1,a], Shu Jie Li [1,a], Kouji Kinoshita [b], Masahito Yamazaki [a, b, c,*]

[a] *Materials Science, Graduate School of Science and Engineering, Shizuoka University, Shizuoka 422-8529, Japan*
[b] *Satellite Venture Business Laboratory, Shizuoka University, Hamamatsu 422-8561, Japan*
[c] *Department of Physics, Faculty of Science, Shizuoka University, 836 Oya, Shizuoka 422-8529, Japan*

Received 23 April 2001; received in revised form 16 August 2001; accepted 30 August 2001

Abstract

The mechanism of the effects of the lanthanum ion (La^{3+}) and the gadolinium ion (Gd^{3+}), which are lanthanides, on the function of membrane proteins and the stability of the membrane structure is not well understood. We investigated the effects of La^{3+} on the stability of the hexagonal II (H_{II}) phase of the phosphatidylethanolamine (PE) membrane at 20°C by small-angle X-ray scattering. As PE membrane we used DPOPE (dipalmitoleoylphosphatidylethanolamine) membrane, which was in the L_α phase in 10 mM PIPES buffer (pH 7.4) at 20°C. An L_α to H_{II} phase transition occurred in the DPOPE membrane at 1.4 mM La^{3+} in 0 M KCl, and at 0.4 mM La^{3+} in 0.5 M KCl and above the critical concentrations the membranes were in the H_{II} phase, indicating that La^{3+} stabilizes the H_{II} phase rather than the L_α phase. The basis vector length, *d*, of DPOPE and DOPE (dioleoylphosphatidylethanolamine) membranes containing 16 wt% tetradecane in excess water condition did not change with an increase in La^{3+} concentration, suggesting that La^{3+} did not change the spontaneous curvature of these PE monolayer membranes. The chain-melting transition temperature of the dielaidoylphosphatidylethanolamine membrane increased with an increase in La^{3+} concentration, indicating that the lateral compression pressure increased. To elucidate the effects of a small percentage of 'guest' lipids with longer acyl chains than the average length of 'host' lipids on the stability of the H_{II} phase, we investigated the effects of the concentration of a guest lipid (DOPE) in a host lipid (DPOPE) membrane on their phase behavior and structure. 12 mol% DOPE induced an L_α to H_{II} phase transition in DOPE/DPOPE membrane, without changing the spontaneous curvature of the monolayer membrane. We found that Ca^{2+} also induced an L_α to H_{II} phase transition in the DPOPE membrane, and compared the effects of Ca^{2+} on PE membranes with those of La^{3+}. Based on these results, we have proposed a new model for the mechanism of the L_α to H_{II} phase transition and the stabilization of the H_{II} phase by La^{3+}.

Keywords: Lanthanum ion; Calcium ion; Acyl chain length; Hexagonal II phase; Spontaneous curvature; Interstitial hydrocarbon region

Abbreviations: DPOPE, 1,2-dipalmitoleoyl-*sn*-glycero-3-phosphatidylethanolamine; DOPE, 1,2-dioleoyl-*sn*-glycero-3-phosphatidylethanolamine; DEPE, 1,2-dielaidoyl-*sn*-glycero-3-phosphatidylethanolamine; H_{II} phase, hexagonal II phase; L_α phase, liquid–crystalline phase; SAXS, small-angle X-ray scattering; MLV, multilamellar vesicle; T_m, chain-melting transition temperature

* Corresponding author, at address c. Fax: +81-54-238-4741.
E-mail address: spmyama@ipc.shizuoka.ac.jp (M. Yamazaki).

[1] These authors contributed equally.

0005-2736/01/$ – see front matter
PII: S0005-2736(01)00413-8

1. Introduction

The lanthanum ion (La^{3+}) and the gadolinium ion (Gd^{3+}), which are lanthanides, are well known to play important roles in the structure and function of biomembranes or phospholipid membranes. In the research field of ionic channel proteins, Gd^{3+} is a well known blocker of the stretch-activated ionic channels (mechanosensitive ionic channels) [1–4], and La^{3+} can modulate the gating properties of the voltage-gated sodium channel [5,6]. These lanthanides also have effects on the structure and stability of phospholipid membranes. Interaction of La^{3+} with the surface of a negatively charged phosphatidylserine (PS) membrane induces effectively the membrane fusion of PS vesicles [7–9]. Moreover, interaction of La^{3+} with the electrical-neutral phosphatidylcholine (PC) membrane induces a conformational change of its head group moving the N end of the P→N vector of the head group toward the water phase, while in the absence of La^{3+} the head group orients almost parallel to the membrane surface, i.e. the P→N vector is extended almost parallel to the membrane surface [10–12]. However, the effects of the interaction of the lanthanides with the membrane interface on the functions of membrane proteins and the stability of the membrane structure are not well understood.

On the other hand, recent findings have renewed the interest in non-bilayer membranes such as the inverted hexagonal (H_{II}) phase and several kinds of cubic phases, since these non-bilayer structures have been postulated to play an important biological role in membrane fusion and in the control of the functions of membrane proteins [13–15]. In most cases, the stability of the H_{II} phase of lipid membranes can be explained by the spontaneous (or intrinsic) curvature of a single monolayer membrane, H_0 [16–18]. According to the definition, inverted curved structures such as the H_{II} phase, where the spontaneous curvature of the monolayer is toward the water region, have a large negative H_0 values. On the other hand, normal structures such as micelles, where the spontaneous curvature of the monolayer is toward the alkyl chain region, have a large positive H_0 values. As the repulsive interaction between the head groups decreases due to electrostatic or steric interaction, the absolute value of H_0 increases in order to decrease the average area of the lipid head group, which makes the H_{II} phase more stable. Thereby, the phase stability of the H_{II} phase of lipid membranes has been determined in most cases by the measurement of the change in the spontaneous curvature of the monolayer membrane due to perturbations such as addition of other components of lipids, temperature, and interaction of solvents with the membrane interface [17–20].

In this report, we investigated the effects of La^{3+} on the stability of the H_{II} phase of the phosphatidylethanolamine (PE) membrane by small-angle X-ray scattering (SAXS). As PE membrane we used DPOPE (1,2-dipalmitoleoyl-*sn*-glycero-3-phosphatidylethanolamine) membrane, which is in the L_α phase in water at 20°C [19]. We found that the L_α to H_{II} phase transition in the membranes occurred at low concentration of La^{3+}, and that La^{3+} stabilizes the H_{II} phase rather than the L_α phase. To consider its mechanism, we performed several kinds of experiments. First, the effect of La^{3+} on the spontaneous curvature of the PE membrane was measured. It was found that La^{3+} did not change the spontaneous curvature. Second, to elucidate the effects of a small percentage of 'guest' lipids with longer acyl chains than the average length of 'host' lipids on the stability of the H_{II} phase, we investigated the effects of the concentration of a guest lipid, 1,2-dioleoyl-*sn*-glycero-3-phosphatidylethanolamine (DOPE) (C18:1), in the host lipid, DPOPE (C16:1), membrane on the phase behavior and structure of DOPE/DPOPE membranes by SAXS. Third, the effect of La^{3+} on the chain-melting temperature of the 1,2-dielaidoyl-*sn*-glycero-3-phosphatidylethanolamine (DEPE) membrane was investigated by differential scanning calorimetry (DSC). Finally, we investigated the effects of Ca^{2+} on the phase stability of DPOPE and DEPE membranes, and compared the effects of Ca^{2+} on PE membranes with those of La^{3+}. Based on these results, we have proposed a new model for the mechanism of the L_α to H_{II} phase transition and the stabilization of the H_{II} phase by La^{3+}.

2. Materials and methods

2.1. Materials and sample preparation

DPOPE, DOPE and DEPE were purchased from

Avanti Polar Lipids. $LaCl_3$ and $CaCl_2$ were purchased from Wako.

Several PE membranes were prepared as follows. Appropriate amounts of phospholipids in chloroform were dried by N_2, and then under vacuum by a rotary pump for more than 12 h. An appropriate amount of 10 mM PIPES buffer (pH 7.4) containing a given concentration of $LaCl_3$ (or $CaCl_2$) was added to these dry lipids in excess solvents (final concentration of lipid is 50 mM), and the suspension was vortexed for about 30 s at room temperature (~20°C) (in the case of DEPE membrane, 50°C) several times. Then, in the case of DEPE membrane, the membrane suspension was sonicated in a bathtub-type sonicator (SHARP, UT-105) for 15 s at room temperature several times. For the measurement of X-ray diffraction, pellets of the suspensions after centrifugation (14 000×*g*, 20 min at 20°C, Tomy, MR-150) were used.

To investigate the structures of DPOPE and DOPE membranes containing 16 wt% tetradecane, we used almost the same method as Chen and Rand [21,22] as follows. (1) To investigate effect of La^{3+} (or Ca^{2+}) on the structures of DPOPE or DOPE membrane, the appropriate amount of DPOPE or DOPE in chloroform was dried by N_2, and then under vacuum by a rotary pump for more than 12 h. Tetradecane was added to the dry lipid by weighing directly. After 48 h incubation at room temperature (~20°C) for equilibration, the appropriate amount of 10 mM PIPES buffer (pH 7.4) containing a given concentration of $LaCl_3$ (or $CaCl_2$) was added to this dry lipid/tetradecane mixture in excess solvents (~7 wt% lipids), and the suspension was vortexed for about 30 s at room temperature (~20°C) several times, and then incubated for another 48 h for equilibration. For the measurement of X-ray diffraction, pellets (or precipitation) of the suspensions after the vortex without centrifugation were used. (2) To investigate the effect of DOPE on the structures of DPOPE membrane, the appropriate amount of the mixture of DPOPE and DOPE in chloroform was dried by N_2, and then under vacuum by a rotary pump for more than 12 h. Tetradecane was added to the dry lipid by weighing directly. After 48 h incubation at room temperature (~20°C) for equilibration, the appropriate amount of 10 mM PIPES buffer (pH 7.4) was added to this dry lipid/tetradecane mixture in excess solvents (~7 wt% lipids), and the suspension was vortexed for about 30 s at room temperature (~20°C) several times, and then incubated for another 48 h for equilibration. For the measurement of X-ray diffraction, pellets (or precipitation) of the suspensions after the vortex without centrifugation were used.

2.2. X-Ray diffraction

X-Ray diffraction experiments were performed using nickel filtered Cu K_α X-rays ($\lambda = 0.154$ nm) from a rotating anode type X-ray generator (Rigaku, Rotaflex, RU-300, 50 kV×300 mA). SAXS data were recorded using a linear (one-dimensional) position sensitive proportional counter (Rigaku, PSPC-5) with a camera length of 350 mm [23,24]. Wide-angle X-ray scattering (WAXS) patterns were recorded by a flat plate film cassette loaded with a highly sensitive X-ray film (Fuji Medical X-ray Film) with a camera length of 45.1 mm. Samples were sealed in a thin-walled glass capillary tube (outer diameter 1.0 mm) and mounted in a thermostatable holder whose stability was ±0.2°C.

2.3. DSC

DSC experiments were performed using a Rigaku DSC-8230B instrument. 50 mM DEPE membrane dispersion was heated at a rate of 2.0°C/min. The chain-melting transition temperatures, T_m, were determined as the onset of the endothermic transition extrapolated to the baseline and also as the maximum of the endothermic transition peak. The details have been described in our previous paper [24].

3. Results

3.1. L_α to H_{II} phase transition in the DPOPE membrane induced by La^{3+}

We investigated the effects of La^{3+} on the phase behavior and structure of DPOPE membranes by X-ray diffraction. SAXS data of the DPOPE membrane in 10 mM PIPES buffer (pH 7.4) at 20°C showed that a set of SAXS peaks had spacings in the ratio of 1:2:3 and the spacing was 4.9 nm (Fig. 1a), in-

dicating that it is in the L_α phase as reported previously [19,25]. At 1.4 mM La^{3+}, a new set of SAXS peaks with a larger spacing was superimposed on the L_α peaks; the new set had spacings in the ratio of $1:\sqrt{3}:2:\sqrt{7}$, which is consistent with a two-dimensional hexagonal (H_{II}) phase (● in Fig. 2). Above 2.0 mM La^{3+}, the L_α peaks disappeared, and the DPOPE membranes were completely in the H_{II} phase (Fig. 1c). At the intermediate concentrations of La^{3+} (1.4–2.0 mM), the two phases coexisted (Fig. 1b).

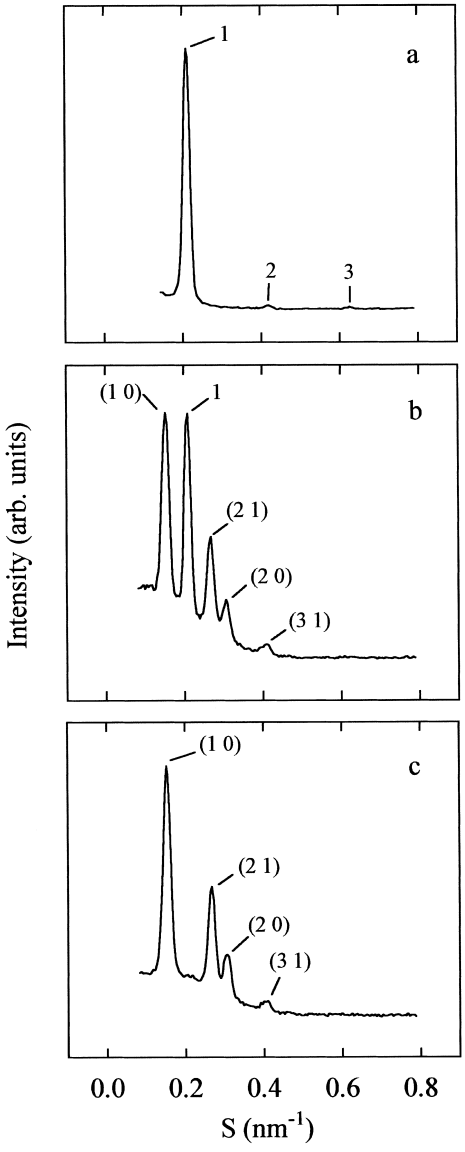

Fig. 1. X-Ray diffraction profile of the DPOPE membrane in various La^{3+} concentrations in 10 mM PIPES buffer (pH 7.4) at 20°C. (a) 0 mM, (b) 1.6 mM, and (c) 3.0 mM La^{3+}.

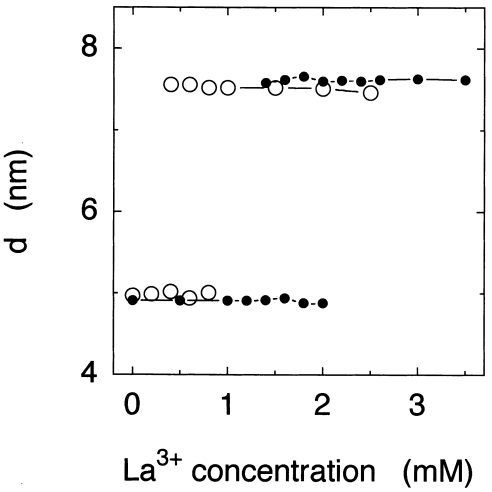

Fig. 2. Spacing or basis vector length, d, of DPOPE membrane in various La^{3+} concentrations at 20°C. ●, in 10 mM PIPES buffer (pH 7.4); ○, in 0.5 M KCl in 10 mM PIPES buffer (pH 7.4). Data with $d \approx 5$ nm correspond to the L_α phase, and those with $d \approx 7.5$ nm correspond to the H_{II} phase.

The basis vector length of the H_{II} phase (center to center distance of adjacent cylinders), d, calculated by $d=(2/\sqrt{3})x$ (x is the spacing in the SAXS), was almost constant ($d=7.6$ nm) with an increase in La^{3+} concentration from 1.4 to 3.5 mM (● in Fig. 2). Hence, La^{3+} induced a transition from L_α to H_{II} phase in the DPOPE membrane at 1.4 mM.

To consider the effects of ionic strength in the bulk phase on this phase transition, we investigated the effects of La^{3+} on the phase behavior and structure of the DPOPE membranes in 10 mM PIPES buffer (pH 7.4) containing 0.5 M KCl (○ in Fig. 2). At 0.4 mM La^{3+}, a new set of SAXS peaks with a larger spacing was superimposed on the L_α peaks; the new set had spacings in the ratio of $1:\sqrt{3}:2:\sqrt{7}$, which is consistent with the H_{II} phase. At and above 1.0 mM La^{3+}, the L_α peaks disappeared, and the DPOPE membranes were completely in the H_{II} phase. Hence, La^{3+} induced a transition from L_α to H_{II} phase in the DPOPE dispersion in 0.5 M KCl at 0.4 mM, which is lower than the critical concentration at which the L_α to H_{II} phase transition occurred in the DPOPE membrane in the absence of KCl.

3.2. *Interaction of La^{3+} with DOPE/tetradecane and DPOPE/tetradecane membranes*

To allow lipid membranes in the H_{II} phase to ex-

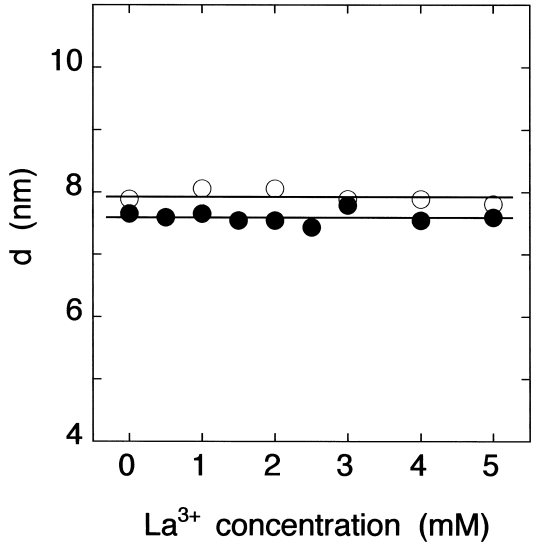

Fig. 3. Basis vector length, d, of DPOPE/tetradecane (○) and DOPE/tetradecane (●) membranes in various La^{3+} concentrations in 10 mM PIPES buffer (pH 7.4) at 20°C. All the membranes were in the H_{II} phase.

press the spontaneous curvature, H_0, addition of alkanes such as decane and tetradecane to the membranes is required because they fill the interstitial region of the H_{II} phase and relax the acyl chain packing stress [16,22,26]. Thereby, to get information on the dependence of the spontaneous curvature of the DOPE membrane on La^{3+} concentration, we investigated the structure of DOPE membrane containing 16 wt% tetradecane in excess water condition [21] in the presence of various concentrations of La^{3+} (● in Fig. 3). The basis vector length, d, of the DOPE/tetradecane membrane in excess water did not change with an increase in La^{3+} concentration.

We also investigated the effect of La^{3+} on the spontaneous curvature of DPOPE membrane containing 16 wt% tetradecane in excess water condition (○ in Fig. 3). In 10 mM PIPES (pH 7.4), the DPOPE membrane was in the L_α phase (Fig. 1a), but the DPOPE membrane containing 16 wt% tetradecane was in the H_{II} phase [19]. As shown in Fig. 3, the basis vector length, d, of the DPOPE/tetradecane membrane in excess water did not change with an increase in La^{3+} concentration.

3.3. *Effect of DOPE concentration on DOPE/DPOPE membrane*

To elucidate the effects of a small percentage of 'guest' lipids with longer acyl chains than the average length of 'host' lipids on the stability of the H_{II} phase, we investigated the effects of the concentration of a guest lipid (DOPE) in host lipid (DPOPE) membrane on their phase behavior and structure by SAXS. The number of carbons in the acyl chain of DOPE ($n=18$) is a little larger than that of DPOPE ($n=16$), and both lipids have a double bond per acyl chain. Hence, the length of the acyl chain of DOPE is a little longer than that of DPOPE.

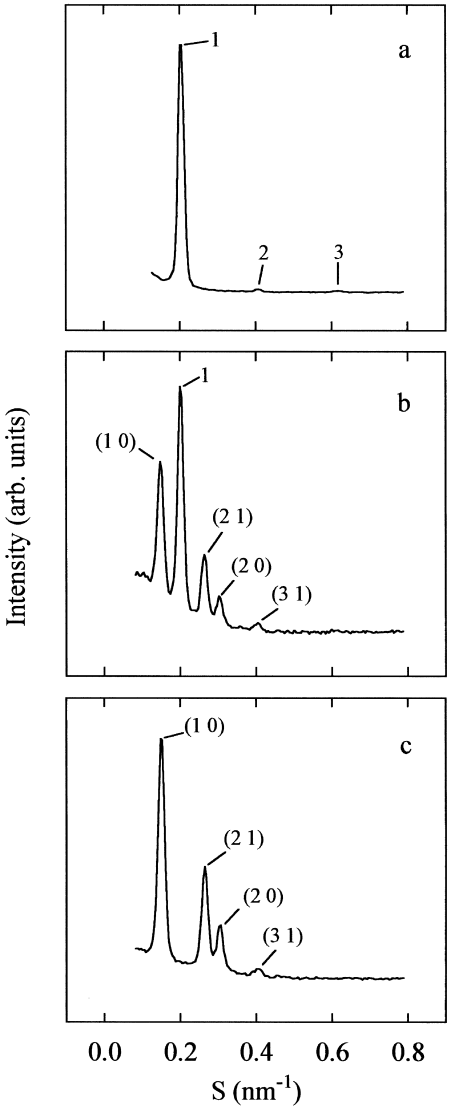

Fig. 4. X-Ray diffraction profile of the DOPE/DPOPE membrane with various DOPE concentrations in 10 mM PIPES buffer (pH 7.4) at 20°C. (a) 8.0 mol%, (b) 20 mol%, and (c) 28 mol% DOPE.

As described in the previous section, the DPOPE membrane in 10 mM PIPES buffer (pH 7.4) at 20°C is in the L_α phase. Addition of small amount of DOPE did not change the phase of the membrane (Fig. 4a). At 12 mol% DOPE, a new set of SAXS peaks with larger spacings was superimposed on the L_α peaks; the new set had spacings in the ratio of $1:\sqrt{3}:2:\sqrt{7}$, which is consistent with the H_{II} phase (Fig. 5). Above 26 mol% DOPE, the L_α peaks disappeared, and the DOPE/DPOPE membranes were completely in the H_{II} phase (Figs. 4c and 5). At the intermediate concentrations of DOPE (12–26 mol%), the two phases coexisted (Fig. 4b). Hence, DOPE induced a phase transition from L_α to H_{II} in the DPOPE membrane at 12 mol%. The basis vector length of the H_{II} phase, d, was almost constant ($d = 7.6$ nm) with an increase in DOPE concentration from 12 to 36 mol% (Fig. 5).

To get information on the dependence of the spontaneous curvature of the DOPE/DPOPE membrane on DOPE concentration, we investigated the structure of DOPE/DPOPE membranes containing 16 wt% tetradecane in the presence of various concentrations of DOPE (Fig. 6). The basis vector length, d,

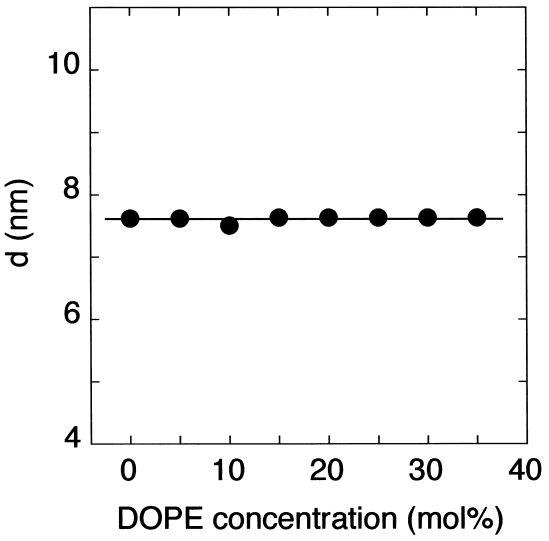

Fig. 6. Basis vector length, d, of the DOPE/DPOPE/tetradecane membranes with various DOPE concentrations in 10 mM PIPES buffer (pH 7.4) at 20°C. All the membranes were in the H_{II} phase.

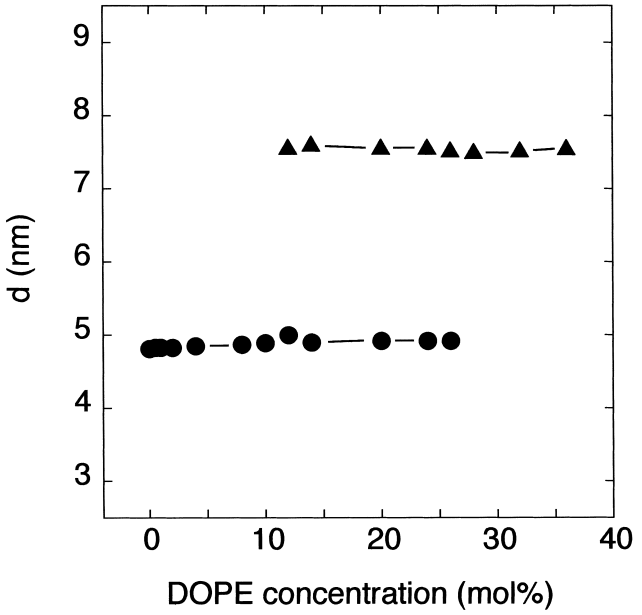

Fig. 5. Spacing or basis vector length, d, of DOPE/DPOPE membranes with various DOPE concentrations in 10 mM PIPES buffer (pH 7.4) at 20°C. ● corresponds to the L_α phase, and ▲ corresponds to the H_{II} phase.

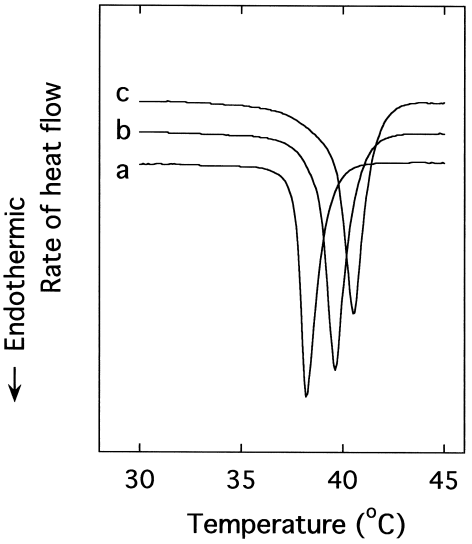

Fig. 7. DSC heating curves of DEPE membrane at various La^{3+} concentrations in 10 mM PIPES buffer (pH 7.4). (a) 0 mM La^{3+}, (b) 4 mM La^{3+}, and (c) 20 mM La^{3+}. Heating rates were 2.0°C/min.

of the DOPE/DPOPE/tetradecane membrane in excess water did not change with an increase in DOPE concentration.

3.4. Effect of La^{3+} on chain-melting transition temperature of DEPE membrane

We investigated the effect of La^{3+} on the chain-melting phase transition (L_β to L_α phase transition) of DEPE membrane by DSC. Fig. 7 shows DSC heating curves of 50 mM DEPE membrane in the presence of various concentrations of La^{3+} in 10 mM PIPES buffer (pH 7.4). In the temperature range in Fig. 7, there was one endothermic peak in each sample, which corresponds to the chain-melting phase transition. As shown in Fig. 8a, the chain-melting phase transition temperature (T_m) increased with an increase in La^{3+} concentration. Figs. 7 and 8a show that broadening of the endothermic peak occurred in the presence of a high concentration of La^{3+}. As shown in Fig. 8b, the increment of T_m in the presence of 0.5 M KCl (▲) at the same La^{3+} concentrations was larger than that in the absence of KCl (●).

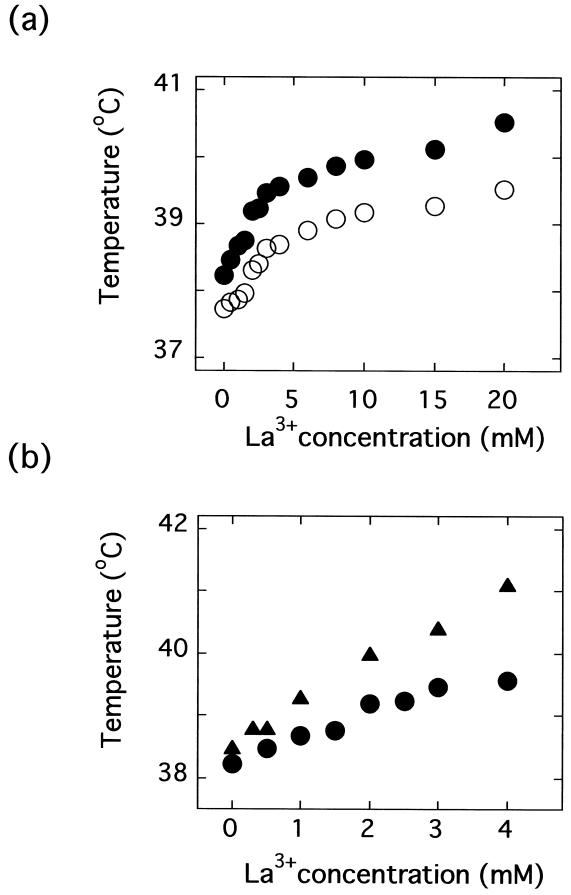

Fig. 8. Dependence of chain-melting transition temperature (T_m) of DEPE membrane on La^{3+} concentration. (a) T_m of DEPE membrane in 10 mM PIPES buffer (pH 7.4). ○ represents the transition onset temperature and ● represents the temperature of the maximum of the endothermic transition peak. (b) T_m of DEPE membrane determined by the temperature of the maximum of the endothermic transition peak in 10 mM PIPES buffer (pH 7.4) (●) and in 10 mM PIPES buffer (pH 7.4) containing 0.5 M KCl (▲) at low concentrations of La^{3+}.

3.5. L_α to H_{II} phase transition in the DPOPE membrane induced by Ca^{2+} and the effect of Ca^{2+} on the chain-melting transition temperature of DEPE membrane

To compare the effect of La^{3+} with that of another ion on the phase stability of PE membranes, we investigated the effects of Ca^{2+} on the phase behavior and structure of DPOPE membranes in 10 mM PIPES buffer (pH 7.4) by X-ray diffraction. At low concentrations of Ca^{2+}, the DPOPE membranes were in the L_α phase (● in Fig. 9). At 48 mM Ca^{2+}, a new set of SAXS peaks with larger spacings (▲ in Fig. 9) was superimposed on the L_α peaks; the new set had spacings in the ratio of $1:\sqrt{3}:2:\sqrt{7}$, which is consistent with the H_{II} phase. Above 70 mM Ca^{2+}, the L_α peaks disappeared, and the DPOPE membranes were completely in the H_{II} phase (Fig. 9). At the intermediate concentrations of Ca^{2+} (48–70 mM), the two phases coexisted. The basis vector length of the H_{II} phase, d, was almost constant ($d = 7.5$ nm) with an increase in La^{3+} concentration from 48 to 100 mM. Hence, Ca^{2+} induced a phase transition from L_α to H_{II} in the DPOPE membrane in 0 M KCl at 48 mM.

To consider the effects of ionic strength in the bulk phase on this phase transition, we investigated the effects of Ca^{2+} on the phase behavior and structure of the DPOPE membranes in 10 mM PIPES buffer (pH 7.4) containing 0.5 M KCl (○ and △ in Fig. 9). At less than 8 mM Ca^{2+}, the membranes were in the L_α phase (○ in Fig. 9). At 8 mM Ca^{2+}, a new set of SAXS peaks with a larger spacing was superimposed on the L_α peaks (△ in Fig. 9); the new set had spacings in the ratio of $1:\sqrt{3}:2:\sqrt{7}$, which is consistent

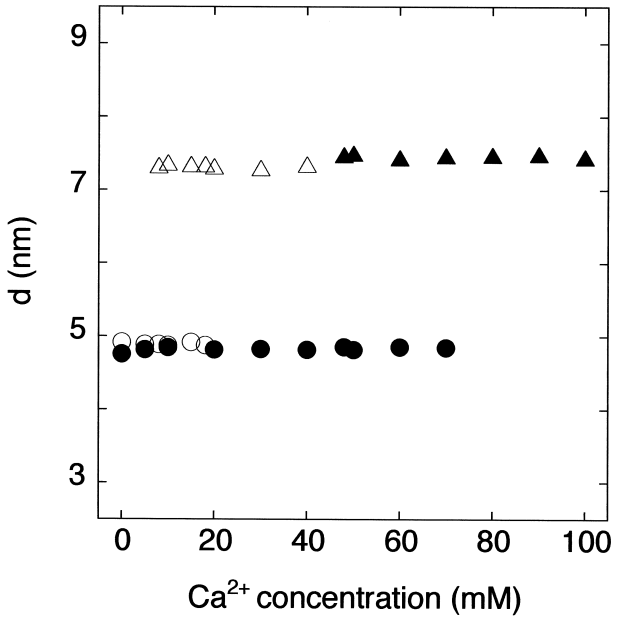

Fig. 9. Spacing or basis vector length, d, of DPOPE membrane in various Ca^{2+} concentrations at 20°C. ●,▲, in 10 mM PIPES buffer (pH 7.4); ○,△, in 0.5 M KCl in 10 mM PIPES buffer (pH 7.4). ● and ○ correspond to the L_α phase, while ▲ and △ correspond to the H_{II} phase.

with the H_{II} phase. Above 20 mM Ca^{2+}, the L_α peaks disappeared, and the DPOPE membranes were completely in the H_{II} phase. Hence, Ca^{2+} induced a phase transition from L_α to H_{II} in the DPOPE membrane in 0.5 M KCl at 8 mM, which is lower than the critical concentration of the L_α to H_{II} phase transition in the DPOPE membrane in 0 M KCl.

To get information on the dependence of the spontaneous curvature of the DPOPE membrane on Ca^{2+} concentration, we investigated the structure of DPOPE membranes containing 16 wt% tetradecane in the presence of various concentrations of Ca^{2+} near the critical concentrations of the L_α to H_{II} phase transitions (Fig. 10). The basis vector length, d, of the DPOPE/tetradecane membrane in excess

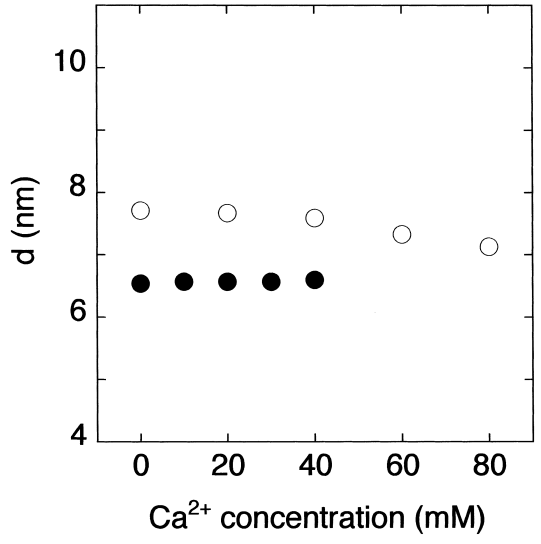

Fig. 10. Basis vector length, d, of the DPOPE/tetradecane membranes in various Ca^{2+} concentrations in 10 mM PIPES buffer (pH 7.4) (○) and in 0.5 M KCl in 10 mM PIPES buffer (pH 7.4) (●) at 20°C. All the membranes were in the H_{II} phase.

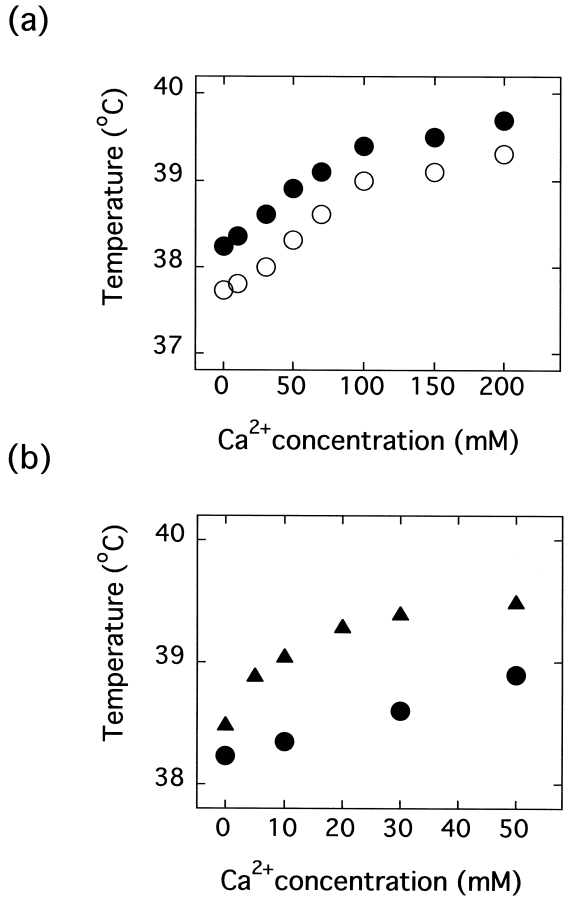

Fig. 11. Dependence of chain-melting phase transition temperature (T_m) of DEPE membrane on Ca^{2+} concentration. (a) T_m of DEPE membrane in 10 mM PIPES buffer (pH 7.4). ○ represents the transition onset temperature and ● represents the temperature of the maximum of the endothermic transition peak. (b) T_m of DEPE membrane determined by the temperature of the maximum of the endothermic transition peak in 10 mM PIPES buffer (pH 7.4) (●) and in 10 mM PIPES buffer (pH 7.4) containing 0.5 M KCl (▲) at low concentrations of Ca^{2+}.

water did not change with an increase in Ca^{2+} concentration near the critical concentration of the L_α to H_{II} phase transition in the presence of 0.5 M KCl (● in Fig. 10), but in the absence of KCl it decreased a little with an increase in Ca^{2+} concentration (○ in Fig. 10).

We also investigated the effect of Ca^{2+} on the chain-melting phase transition of DEPE membrane by DSC. As shown in Fig. 11a, the chain-melting phase transition temperature (T_m) of 50 mM DEPE membrane in 10 mM PIPES buffer (pH 7.4) increased with an increase in Ca^{2+} concentration. Fig. 11b shows that the increase in T_m in the presence of 0.5 M KCl at the same Ca^{2+} concentrations was larger than that in the absence of KCl.

4. Discussion

4.1. La^{3+} stabilizes the H_{II} phase rather than the L_α phase

The results in Fig. 2 clearly indicate that the L_α to H_{II} phase transitions occurred in the DPOPE membrane at 20°C at low concentrations of La^{3+}, and that the presence of 0.5 M KCl decreases the critical concentration of La^{3+} for the L_α to H_{II} phase transition. Thereby, La^{3+} stabilizes the H_{II} phase rather than the L_α phase. What is the mechanism of this phase transition?

Generally, the difference of the chemical potential of the phospholipid membrane in the H_{II} phase (μ^{HII}) and the bilayer liquid–crystalline (L_α) phase (μ^{bil}), $\Delta\mu$, is expressed as follows [27,28]:

$$\begin{aligned}\Delta\mu &= \mu^{HII}-\mu^{bil}\\ &= (\mu^{HII}_{curv}-\mu^{bil}_{curv})+(\mu^{HII}_{ch}-\mu^{bil}_{ch})\\ &= \Delta\mu_{curv}+\Delta\mu_{ch}\end{aligned} \quad (1)$$

where $\Delta\mu_{curv}$ is a term due to the curvature elastic energy (or curvature energy), and $\Delta\mu_{ch}$ is a term due to interstitial chain packing of the H_{II} phase. The spontaneous (or intrinsic) curvature of a single monolayer membrane, H_0, is a useful parameter characterizing non-bilayer membranes, which is expressed as $H_0 = 1/R_0$, where R_0 is the radius of the spontaneous curvature [16–18]. Using R_0, the curvature energy of the H_{II} phase, μ_{curv}, in Eq. 1 is expressed as [18,29]:

$$\mu_{curv} = \frac{1}{2}(N_A \kappa A_o)\left(\frac{1}{R_w}-\frac{1}{R_0}\right)^2 \quad (2)$$

where N_A is Avogadro's number, κ is the elastic bending modulus of the monolayer membrane, A_o is the equilibrium surface area per lipid molecule in the membrane, R_w is the radius of curvature of the lipid monolayer. In excess water, the membrane in the H_{II} phase has a curvature close to the spontaneous curvature to minimize the curvature energy, whereby $R_w \approx R_0$. For convenience, we assume $\mu^{HII}_{curv} = 0$ in excess water. Since $1/R_w = 0$ in L_α phase,

$$\Delta\mu_{curv} = (\mu^{HII}_{curv}-\mu^{bil}_{curv}) = -\frac{1}{2}\frac{N_A \kappa A^{bil}_o}{R_0^2} \ (<0) \quad (3)$$

where A^{bil}_o is the optimal surface area per lipid molecule of the L_α phase. Eq. 3 shows that $\Delta\mu_{curv}$ is always negative ($\Delta\mu_{curv} < 0$), thereby it is an important factor stabilizing the H_{II} phase. On the other hand, in the H_{II} phase, acyl chains of lipids have to extend to different lengths to fill the interstitial hydrocarbon region, which decreases the entropy of chains and increases the free energy of the membrane [27]. Therefore, this packing energy of the acyl chains unstabilizes the H_{II} phase, and thus $\Delta\mu_{ch}$ is always positive ($\Delta\mu_{ch} > 0$). The addition of alkanes such as decane and tetradecane to the membrane decreases $\Delta\mu_{ch}$, because the alkanes fill the interstitial region of the H_{II} phase and relax the acyl chain packing stress [16,22,26]. In most cases, phase transitions between the H_{II} and the L_α phases are determined by the interplay of these two factors, $\Delta\mu_{curv}$ and $\Delta\mu_{ch}$.

Eq. 3 shows that the absolute value of $\Delta\mu_{curv}$ increases with a decrease in R_0 and the change in the spontaneous curvature induces a change in the stability of the H_{II} phase. The result of Fig. 3 gives information on the change of the radius of the spontaneous curvature R_0 of the DOPE and DPOPE membranes. The basis vector length of the H_{II} phase, d, is expressed as the sum of the radius of the water tube, R_w, and the thickness of the monolayer membrane, d_l, i.e. $d = 2(R_w + d_l)$ [16,17]. In excess water, the DOPE or DPOPE membrane containing 16 wt% tetradecane in the H_{II} phase has a curvature of H_0 to minimize the curvature free energy, and thereby, $R_w = R_0$. No change in d of the DOPE/tetradecane

and DPOPE/tetradecane membranes induced by La^{3+} is attributed to no change in R_w, since the change in d_l is assumed to be small. Thus, the result of Fig. 3 indicates that the spontaneous curvature of these PE membranes did not change with an increase in La^{3+} concentration, and thereby, the La^{3+}-induced L_α to H_{II} phase transition is not due to the change in the spontaneous curvature.

4.2. The mechanism of the L_α to H_{II} phase transition induced by La^{3+}

The effect of La^{3+} on the physical properties of PC membranes has been investigated by several techniques. The solid NMR method (^{2}H-NMR) revealed that La^{3+} can bind with the head groups of electrical-neutral PC membranes near the phosphate group of the head groups and induce a conformational change of the head group moving the N end of the P→N vector of the head groups toward the water phase, while in water in the absence of these ions the head groups orient almost parallel to the membrane surface, i.e. the P→N vector of the head groups is extended almost parallel to the membrane surface [10,11,30]. For PE membranes in water, their head groups orient almost parallel to the membrane surface, i.e. the P→N vector of the head groups is extended almost parallel to the membrane surface [31]. We can reasonably assume that a similar conformational change of the head group of the electrical-neutral PE membrane is induced by La^{3+}. This conformational change decreases the steric repulsive interaction between the head groups in the phospholipid membrane, Π_{head}. The binding of La^{3+} with the head groups of the PE membranes may also induce an electrostatic attraction between the negative charges of the phosphate groups (O^-) of neighboring phospholipids. Otherwise, the conformational change of the head group is difficult, because its conformation in the absence of La^{3+} is more energetically favorable than that in the presence of La^{3+} from the point of the electrostatic interaction energy between the dipole moments of neighboring phospholipid head groups. This attraction also decreases the repulsive interaction between the head groups. In equilibrium, three kinds of lateral pressures in the membrane have to balance, i.e. $\Pi_{head}+\Pi_{chain}=\gamma$, where Π_{chain} is the repulsive chain pressure, and γ is the attractive interfacial pressure due to the hydrophobic interaction between the acyl chains and water at the membrane surface [32]. We can assume that γ is almost constant in the presence of low concentrations of La^{3+}. Therefore, the lateral compression pressure of the membrane, $\gamma-\Pi_{head}$, at the local place of the membrane near the binding site of La^{3+} becomes larger than that of the original DPOPE membrane in the absence of La^{3+}. This can reasonably explain the increase in the chain-melting transition temperature, T_m, of the DEPE membrane and the decrease of cooperativity in the phase transition (Figs. 7 and 8). Similar situations that the increase in the lateral compression pressure induces an increase in T_m were observed in other systems [25,33,34]. However, the binding of La^{3+} on the membrane surface of the DEPE membrane increases the surface charge density, which has an effect of decreasing T_m due to the electrostatic repulsive interaction [35,36]. Therefore, in this case, the effect of the lateral pressure on T_m (i.e. the increase in T_m) is a prevailing effect over that of the electrostatic interaction due to the surface charge on T_m (i.e. the decrease in T_m). This is the same situation as the low pH-induced increase in T_m of the dihexadecylphosphatidylcholine (DHPC) membrane [34].

The local lateral compression pressure due to the binding of La^{3+} on the PE membrane can induce the ordering of the conformation of the acyl chains and thereby extend the chains of the PE molecules of that local place. The percentage of PE lipids with longer acyl chains than the original average length of these lipids in the membranes increases with an increase in La^{3+} concentration.

We propose a model for the mechanism of the L_α to H_{II} phase transition induced by La^{3+} in the DPOPE membranes and the stabilization of the H_{II} phase of PE membrane by La^{3+}. As described above, the packing energy of the acyl chains unstabilizes the H_{II} phase, and thus $\Delta\mu_{ch}$ is always positive ($\Delta\mu_{ch}>0$). The small percentage of PE lipids with longer acyl chains than the average length produced by the small amount of La^{3+} will be localized at the region where their acyl chains can fill the interstitial hydrocarbon region in the H_{II} phase membrane. This can decrease the packing energy of the acyl chains in the H_{II} phase, and thereby decreases $\Delta\mu_{ch}$. At the critical concentration of La^{3+}, i.e. at the critical con-

centration of the lipids with longer acyl chains, L_α to H_{II} phase transition occurs. In brief, the La^{3+}-induced L_α to H_{II} phase transition occurs not by the change in the spontaneous curvature of the monolayer membrane, but by the change in the chain packing energy at the interstitial region of the H_{II} phase. Addition of alkanes such as tetradecane to the DPOPE membrane induced the L_α to H_{II} phase transition (Fig. 3 and [19]), indicating that the decrease in packing energy of acyl chains in the interstitial region of the H_{II} phase induced this phase transition. It also supports our new model.

In the presence of a high concentration of NaCl or KCl, the binding of La^{3+} on the PE membrane is much enhanced due to the screening of the positive surface charge of the membrane produced by the binding of La^{3+}. In the case of PC membrane, this is proved by the solid NMR experiments [11]. This increase in the amount of the bound La^{3+} on the membrane can reasonably explain two effects of the presence of 0.5 M KCl; one is that it decreases the critical concentration of La^{3+} for the L_α to H_{II} phase transition of the DPOPE membrane (Fig. 2) and the other is that it increases the increment of the chain-melting transition temperature (T_m) of the DEPE membrane due to the La^{3+} (Fig. 8). As described above, the L_α to H_{II} phase transition and the increase in T_m are induced by the lateral compression pressure of the membrane due to the binding of La^{3+} on the membrane. Based on our new model, we can reasonably conclude that the amount of the bound La^{3+} on the membrane determines the L_α to H_{II} phase transition and the increase in T_m, and thereby, the critical concentration of La^{3+} for the L_α to H_{II} phase transition induces almost the same increase in T_m under various conditions. The validity of this conclusion can be checked quantitatively as follows. In 0 M KCl, T_m of the DEPE membrane at the critical concentration of La^{3+} inducing the L_α to H_{II} phase transition of the DPOPE membrane (i.e. 1.4 mM La^{3+}) is higher than T_m in the absence of La^{3+} by 0.5 ± 0.1°C (i.e. $\Delta T_m = 0.5 \pm 0.1$°C). In 0.5 M KCl, T_m of the DEPE membrane at the critical concentration of La^{3+} inducing the L_α to H_{II} phase transition of the DPOPE membrane (i.e. 0.4 mM La^{3+}) is higher than T_m in the absence of La^{3+} by 0.3 ± 0.1°C (i.e. $\Delta T_m = 0.3 \pm 0.1$°C). Here we used values of T_m which were determined by the maximum of the endothermic transition peak. These results support the above conclusion.

4.3. The mechanism of the L_α to H_{II} phase transition induced by the addition of DOPE to the DPOPE membrane

To verify our model for the mechanism of the L_α to H_{II} phase transition described above, we investigated the effects of a small percentage of 'guest' lipids with longer acyl chains than the average length of 'host' lipids on the stability of the H_{II} phase (Fig. 5). The result of Fig. 5 clearly shows that the incorporation of the guest PE molecule (DOPE) with longer acyl chains than that of the host PE molecule (DPOPE) induces the L_α to H_{II} phase transition, and thereby it stabilizes the H_{II} phase rather than the L_α phase. The DOPE membrane is in the H_{II} phase at 20°C, and thereby, the incorporation of DOPE into the DPOPE membrane may have another effect on the structure and physical property of the membrane than the variation of the acyl chain length. For example, when the DOPE concentration increased in the dioleoyl-PC (DOPC) membrane, L_α to H_{II} phase transition occurred at the critical concentration of DOPE [18,26]. In this case, the radius of the spontaneous curvature of the DOPE/DOPC membrane largely decreased with an increase in DOPE concentration [18,26], which is the main reason for the phase transition. On the other hand, in the DOPE/DPOPE membrane the radius of the spontaneous curvature did not change (Fig. 6). The L_α to H_{II} phase transition induced by the incorporation of DOPE can be reasonably explained as follows. As described above, in the H_{II} phase, acyl chains of a small fraction of lipids have to extend to fill the interstitial hydrocarbon region, which increases the free energy of the membrane. Therefore, this packing energy of the acyl chains unstabilizes the H_{II} phase, and thus $\Delta\mu_{ch}$ is always positive ($\Delta\mu_{ch} > 0$). When lipid membrane contains a small percentage of lipids with longer acyl chains than the average length of host lipids, they will be localized at the region where their acyl chains can fill the interstitial hydrocarbon region in the H_{II} phase membrane. This can decrease the packing energy of the acyl chains in the H_{II} phase, thereby decreasing $\Delta\mu_{ch}$. At the critical concentration of the lipids with

longer acyl chains, L_α to H_{II} phase transition occurs. This result supports our model for the mechanism of the La^{3+}-induced L_α to H_{II} phase transition in the DPOPE membrane and the stabilization of the H_{II} phase by La^{3+}.

4.4. Comparison of the effects of La^{3+} and Ca^{2+} on phase stability of PE membranes

The results in Fig. 9 clearly indicate that the L_α to H_{II} phase transitions occurred in the DPOPE membrane at 20°C at low concentrations of Ca^{2+}, and that the presence of 0.5 M KCl decreases the critical concentration of Ca^{2+} for the L_α to H_{II} phase transition. Thereby, Ca^{2+} also stabilizes the H_{II} phase rather than the L_α phase. The critical concentrations of Ca^{2+} inducing the L_α to H_{II} phase transition were more than 10 times the critical concentrations of La^{3+} under the same condition. The result of Fig. 10 suggests that the spontaneous curvature of these PE membranes did not change largely with an increase in Ca^{2+} concentration. The chain-melting transition temperature (T_m) of the DEPE membrane also increased with an increase in Ca^{2+} concentration, but the effect of Ca^{2+} on T_m was much smaller than that of La^{3+} (Fig. 11). Therefore, the main mechanism of the Ca^{2+}-induced L_α to H_{II} phase transition of the DPOPE membrane is almost the same as that of the La^{3+}-induced phase transition described above: the lateral compression pressure due to the binding of Ca^{2+} on the membrane is one of the main reasons for the L_α to H_{II} phase transition.

As described in the effects of La^{3+}, based on our model, we can reasonably conclude that the amount of the bound Ca^{2+} on the membrane determines the L_α to H_{II} phase transition and the increase in T_m. We check its validity quantitatively. In 0 M KCl, T_m of the DEPE membrane at the Ca^{2+} concentration inducing the L_α to H_{II} phase transition of the DPOPE membrane (i.e. 50 mM Ca^{2+}) is higher than T_m in the absence of Ca^{2+} by 0.7 ± 0.1°C (i.e. $\Delta T_m = 0.7 \pm 0.1$°C). In 0.5 M KCl, T_m of the DEPE membrane at the Ca^{2+} concentration inducing the L_α to H_{II} phase transition of the DPOPE membrane (i.e. 8 mM Ca^{2+}) is higher than T_m in the absence of Ca^{2+} by 0.6 ± 0.1°C (i.e. $\Delta T_m = 0.6 \pm 0.1$°C). These results show that the critical concentrations of Ca^{2+} of the L_α to H_{II} phase transition induced almost the same increase in T_m in both KCl concentrations. This supports the above conclusion. The values of ΔT_m in the case of Ca^{2+} are almost the same as those in the case of La^{3+}. This suggests that, irrespective of the kinds of ions (La^{3+} and Ca^{2+}), there is a correlation between the increase in T_m due to the binding of ions and the ion-induced L_α to H_{II} phase transition.

The experimental results in this report also show that the efficiency of Ca^{2+} in inducing the L_α to H_{II} phase transition and the increase in T_m is much lower than that of La^{3+}. We consider two reasons for this. One is that the lateral compression pressure of the membrane induced by a bound Ca^{2+} is weaker than that of a bound La^{3+}. The other is that the binding constant of Ca^{2+} on PE membrane is smaller than that of La^{3+}, which is the same tendency as in the interaction of these ions with PC membrane. In the case of DPPC membrane in the L_α phase (at 59°C), the apparent binding constants of $K = 120$ M^{-1} for La^{3+} and $K = 19$ M^{-1} for Ca^{2+} were determined by the analysis of the deuterium quadrupole splittings obtained by the solid NMR method [11].

To prove our model for the mechanism of the L_α to H_{II} phase transition, we need more experiments and quantitative analysis in the future. It is necessary to obtain more direct experimental evidence supporting the lengthening of the acyl chains of PE membranes due to the binding of ions, such as the measurement of an order parameter of the acyl chains. In the interaction of Ca^{2+} with the DPOPE membrane in 0 M KCl, the radius of the spontaneous curvature of the membrane may decrease a little (○ in Fig. 10). Thereby, in this case, both effects, i.e. the lengthening of the acyl chains and the increase of the spontaneous curvature, may play an important role in the L_α to H_{II} phase transition. To compare the roles of these two effects quantitatively, we have to develop a method to calculate the interstitial chain packing energy quantitatively by experimental data.

4.5. Biological implication

So far, the spontaneous curvature of the monolayer membrane has been considered to play an important role in the stability of the H_{II} phase [17–19] and cubic phases [20,37]. However, the results of this

report suggest that the distribution of the length of lipid acyl chains would change the stability of non-bilayer membranes. We can generalize the mechanism of the La^{3+}-induced L_α to H_{II} phase transition; the production of a small percentage of lipids with longer acyl chains than the original average length of the lipids in the membrane can induce an L_α to H_{II} phase transition, or at least produce a membrane with high negative curvature. We expect that interaction of proteins or peptides with lipid membranes can induce an L_α to H_{II} phase transition by this mechanism, and that in cells, the production (or synthesis) of lipids with longer acyl chains than the original average length of the lipids in the membrane may play an important role in the production of a membrane with high negative curvature. Siegel and Epand recently reported that the influenza hemagglutinin fusion peptide (20-mer) induced a cubic phase in the DPOPE membrane without a change in the spontaneous curvature, suggesting that a factor other than the spontaneous curvature is important in the formation of cubic phases of biomembranes [38]. Moreover, the increase in the lateral compression pressure and the extension of the acyl chains at the local place of the membrane play an important role in the control of functions of membrane proteins such as the stretch-activated ionic channels and the voltage-gated ionic channels. Further research on our new model is necessary.

Acknowledgements

This research was supported partly by a grant from the Asahi Glass Foundation to M.Y.

References

[1] M. Gustin, X.-L. Zhou, B. Martinac, C. Kung, Science 242 (1988) 762–765.
[2] X.-C. Yang, F. Sachs, Science 243 (1989) 1068–1071.
[3] X.-L. Zhou, C. Kung, EMBO J. 11 (1992) 2869–2875.
[4] J. Lee, A. Ishihama, G. Oxford, B. Johnson, K. Jacobson, Nature 400 (1999) 382–386.
[5] M. Takata, W.F. Pickard, J.Y. Lettvin, J.W. Moore, J. Gen. Physiol. 50 (1966) 461–471.
[6] C.M. Armstrong, G. Cota, J. Gen. Physiol. 96 (1990) 1129–1140.
[7] M.M. Hammoudah, S. Nir, T. Isac, R. Kornhauser, T.P. Stewart, S.W. Hui, W.L.C. Vaz, Biochim. Biophys. Acta 558 (1979) 338–343.
[8] J. Bentz, D. Alford, J. Cohen, N. Düzgünes, Biophys. J. 53 (1988) 593–607.
[9] M. Petersheim, J. Sun, Biophys. J. 55 (1989) 631–636.
[10] M.F. Brown, J. Seelig, Nature 269 (1977) 721–723.
[11] H. Akutsu, J. Seelig, Biochemistry 20 (1981) 7366–7373.
[12] J. Seelig, P.M. Macdonald, P.G. Scherer, Biochemistry 26 (1987) 7535–7541.
[13] B. de Kruijff, Nature 386 (1997) 129–130.
[14] V. Luzzati, Curr. Opin. Struct. Biol. 7 (1997) 661–668.
[15] G. Basáñez, J.L. Nieva, E. Rivas, A. Alonso, F.M. Goñi, Biophys. J. 70 (1996) 2299–2306.
[16] S.M. Gruner, Proc. Natl. Acad. Sci. USA 82 (1985) 3665–3669.
[17] M.W. Tate, S.M. Gruner, Biochemistry 28 (1989) 4245–4253.
[18] D. Marsh, Biophys. J. 70 (1996) 2248–2255.
[19] K. Kinoshita, S.J. Li, M. Yamazaki, Eur. Biophys. J. 30 (2001) 207–220.
[20] S.J. Li, Y. Yamashita, M. Yamazaki, Biophys. J. 81 (2001) 983–993.
[21] Z. Chen, R.P. Rand, Biophys. J. 73 (1997) 267–276.
[22] Z. Chen, R.P. Rand, Biophys. J. 74 (1998) 944–952.
[23] O. Glatter, O. Kratky, Small Angle X-ray Scattering, Academic Press, New York, 1982.
[24] M. Yamazaki, M. Ohshika, N. Kashiwagi, T. Asano, Biophys. Chem. 43 (1992) 29–37.
[25] A. Colotto, I. Martin, J.-M. Ruysschaert, A. Sen, S.W. Hui, R.P. Epand, Biochemistry 35 (1996) 980–989.
[26] R.P. Rand, N.L. Fuller, S.M. Gruner, V.A. Parsegian, Biochemistry 29 (1990) 76–87.
[27] D.M. Anderson, S.M. Gruner, S. Leibler, Proc. Natl. Acad. Sci. USA 85 (1988) 5364–5368.
[28] S.M. Gruner, J. Phys. Chem. 93 (1989) 7562–7570.
[29] G.L. Kirk, S.M. Gruner, D.L. Stein, Biochemistry 23 (1984) 1093–1102.
[30] H. Akutsu, T. Nagamori, Biochemistry 30 (1991) 4510–4516.
[31] M.F. Brown, J. Seelig, Biochemistry 17 (1978) 381–384.
[32] J.N. Israelachvili, Intermolecular and Surface Forces, 2nd edn., Academic Press, New York, 1992.
[33] K. Kinoshita, S. Furuike, M. Yamazaki, Biophys. Chem. 74 (1998) 237–249.
[34] S. Furuike, V.G. Levadny, S.J. Li, M. Yamazaki, Biophys. J. 77 (1999) 2015–2023.
[35] H. Träuble, M. Teubner, P. Woolley, H. Eibl, Biophys. Chem. 4 (1976) 319–342.
[36] F. Jähnig, K. Harlos, H. Vogel, H. Eible, Biochemistry 18 (1979) 1459–1468.
[37] Y. Aota-Nakano, S.J. Li, M. Yamazaki, Biochim. Biophys. Acta 1461 (1999) 96–102.
[38] D.P. Siegel, R.M. Epand, Biochim. Biophys. Acta 1468 (2000) 87–98.